

FlowTime: Towards Continuous Generative Watch Time Prediction via Flow-based Personalized Priors

Hongxu Ma^{*†}
Fudan University
Shanghai, China
hxma24@m.fudan.edu.cn

Han Zhou^{*}
Shanghai University of
Finance and Economics
Shanghai, China
zhouhan@stu.sufe.edu.cn

Chenghou Jin^{*}
Fudan University
Shanghai, China
jinch24@m.fudan.edu.cn

Jie Zhang
Kuaishou Technology
Beijing, China
zhangjie39@kuaishou.com

Xiaoyu Yang
Kuaishou Technology
Beijing, China
yangxiaoyu@kuaishou.com

Chunjie Chen
Kuaishou Technology
Beijing, China
chencj517@gmail.com

Jihong Guan
Tongji University
Shanghai, China
jhguan@tongji.edu.cn

Shuigeng Zhou[‡]
Fudan University
Shanghai, China
sgzhou@fudan.edu.cn

Abstract

Watch time has emerged as a pivotal metric for optimizing deep user engagement in short-video recommender systems. However, current methods of watch time prediction (WTP) suffer from inherent paradigm-specific limitations. *Direct Regression* faces mean-collapse due to unimodal Gaussian assumptions, while *Ordinal Regression* is hampered by quantization errors from rigid discretization. Similarly, *Discrete Generative Regression* struggles with high inference latency and heuristic vocabulary design. Beyond these specific flaws, a shared deficiency is the inability to capture the intrinsic multimodality and heterogeneity of *User-Item Interaction Patterns*.

To address these challenges, we first revisit the WTP problem from a causal perspective, and identify these user-specific patterns as structural confounders that modulate watch time outcomes, where identical interests manifest as distinct watch time outcomes conditioned on diverse user habits. Then, we formally propose a new (or the fourth) paradigm — **Continuous Generative Regression**, and introduce **FlowTime**, a novel method utilizing a One-step Generative Variational Autoencoder. FlowTime effectively circumvents the latency of iterative denoising while maintaining the expressivity of continuous latent spaces. Furthermore, we design a *Flow-based Personalized Prior* that leverages NFs to warp a standard Gaussian prior into a complex, history-conditioned manifold, thereby enabling the adaptive modeling of multimodal interaction patterns. Finally, we build *TimeRec*, the first open-source WTP Library, alongside a novel personalization metric to establish a rigorous benchmarking standard. Extensive offline experiments and online A/B tests demonstrate FlowTime’s significant superiority over SOTA methods. Our code is available at <https://github.com/snailma0229/TimeRec.git>.

^{*}Both authors contributed equally to this research.

[†]Work done during the internship at Kuaishou Technology.

[‡]Corresponding author.



CCS Concepts

• **Information systems** → *Recommender systems*.

Keywords

Recommendation, Watch-time prediction, Generative Modeling

ACM Reference Format:

Hongxu Ma, Han Zhou, Chenghou Jin, Jie Zhang, Xiaoyu Yang, Chunjie Chen, Jihong Guan, and Shuigeng Zhou. 2026. FlowTime: Towards Continuous Generative Watch Time Prediction via Flow-based Personalized Priors. In *Proceedings of the 32nd ACM SIGKDD Conference on Knowledge Discovery and Data Mining V.2 (KDD '26)*, August 09–13, 2026, Jeju Island, Republic of Korea. ACM, New York, NY, USA, 12 pages. <https://doi.org/10.1145/3770855.3818143>

1 Introduction

As short-video platforms increasingly dominate global information consumption [2, 3, 24, 25], the objective of recommender systems is shifting from traditional Click-Through Rate (CTR) to deeper engagement-centric metrics [6, 7], epitomized by *Watch Time*. Serving as a pivotal proxy for user satisfaction and immersion, accurate *watch time prediction* (WTP) is critical for optimizing traffic allocation, enhancing user retention and further driving revenue growth [2, 34, 38].

WTP techniques evolves through three paradigms, each constrained by its specific limitations: (1) *Direct Regression* using MSE-based optimization implicitly assumes a unimodal Gaussian prior, leading to mean-collapse on complex distributions — a deficiency that remains unrectified despite causal debiasing [11, 40, 42, 43]. (2) *Ordinal Regression* discretizes time for interval-wise classification [1, 21, 29, 33] but suffers from rigid quantization granularity and the erroneous assumption of conditional independence among intervals. (3) *Discrete Generative Regression* adapts language modeling to generate quantized tokens [26], yet is hampered by heuristic vocabulary design and high latency from autoregressive decoding.

Apart from these paradigm-specific limitations, a shared challenge lies in the intrinsic multimodality and heterogeneity of watch time distributions [44]. From a causal perspective, traditional WTP techniques simply assume that WTP is solely determined by user interest as shown in Fig. 1(a). Actually, WTP is not merely a function of interest, but influenced by the interplay between interest and *User-Item Interaction Patterns*, which act as structural confounders

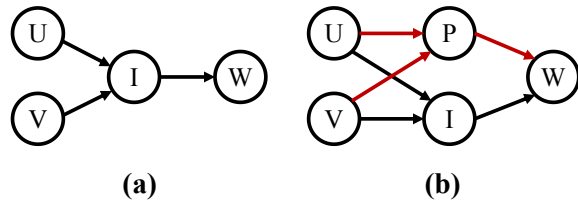


Figure 1: Causal graphs for WTP. Nodes: U -User, V -Video, I -Interest, P -Interaction Pattern, and W -Watch Time. (a) The traditional view. (b) We identify interaction patterns (P) as structural confounders (red lines) to modulate outcomes.

in Fig. 1(b). For example, as shown in Fig. 2 (a), given the same interest, an “aggressive” user exhibits a bimodal distribution (immediate skip vs. completion), whereas a “passive” user generates a unimodal distribution (hovering). Similarly, Fig. 2 (b) illustrates analogous variations driven by distinct item characteristics. This implies that identical interests map to distinct distribution topologies conditioned on user-item patterns, ultimately leading to divergent watch time outcomes. However, prior works largely neglect such pattern-driven distribution shifts, failing to capture personalized multimodal distributions and limiting predictive fidelity.

To address the limitations above, inspired by the success of generative models [9, 13, 22] in modeling intricate data manifolds, we formally propose the **Continuous Generative Regression Paradigm**, which allows for directly fitting complex, multimodal watch time distributions. However, adapting this paradigm to watch time modeling in recommender systems faces two critical hurdles:

1. *Inference Latency*: The iterative denoising mechanism of mainstream generative models, such as diffusion models [9], conflicts with the stringent latency constraints of online systems.
2. *Prior Mismatch*: The standard Gaussian prior underlying vanilla generative models fails to capture the highly heterogeneous and personalized user-item behavioral patterns.

In response, we propose **FlowTime**, a novel continuous generative framework. For latency, we adopt a One-step Variational Autoencoder (VAE) architecture, bypassing costly iterative processes to ensure real-time inference efficiency [16, 17] while learning continuous latent space to maintain expressive power [45]. To address prior mismatch, we design a *Flow-based Personalized Prior*. Conditioned on historical user-item interaction patterns, we leverage NFs to learn bijective transformations that warp the generic Gaussian latent space into a pattern-specific prior manifold. This personalized topology enables adaptively capturing diverse and complex preference distributions, thereby establishing more accurate ordinal relationships for precise WTP. Extensive offline and online experiments demonstrate the superiority of our approach across standard accuracy and ranking metrics, as well as our proposed novel metric to quantify personalization fidelity.

Furthermore, to address widespread inconsistencies in data preprocessing and evaluation protocols, we construct the field’s first open-source Watch-Time Prediction Library—*TimeRec*. By standardizing evaluation protocols and integrating reproduced SOTA methods, TimeRec provides a rigorous baseline for fair and consistent benchmarking [35].

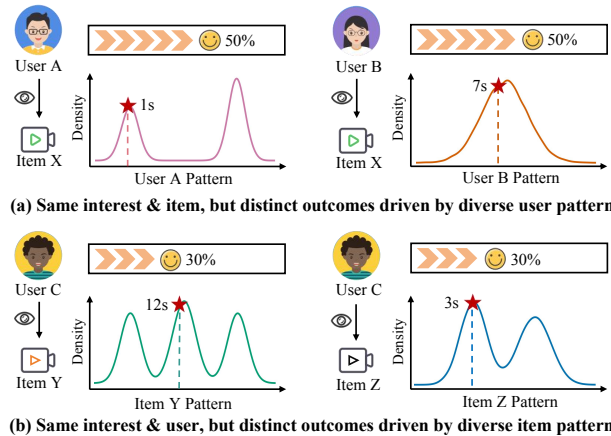


Figure 2: Impact of interaction patterns on watch time. Predictions for identical interest levels diverge based on (a) user habits and (b) item characteristics, highlighting the necessity of pattern-aware modeling.

The main contributions are summarized as follows:

- We formally propose *Continuous Generative Regression* as a new paradigm for WTP. From a causal perspective, we identify the structural modulation of user-item patterns on WTP, and provide the theoretical superiority of this paradigm in overcoming the intrinsic limitations of traditional regression and discretization paradigms.
- We introduce FlowTime, the first framework for the new paradigm. By integrating One-step Generation with a Flow-based Personalized Prior, it reshapes the prior space into pattern-driven manifolds, achieving precise and adaptive modeling of heterogeneous patterns without sacrificing inference efficiency.
- Extensive offline experiments and online A/B tests demonstrate that FlowTime significantly outperforms existing state-of-the-art methods. We also provide in-depth analysis of key factors and underlying mechanisms driving the performance gains..
- Last but not least, we build the first open-source WTP Library *TimeRec*. Integrating our novel personalization metric, this toolkit provides a rigorous baseline for fair and consistent benchmarking.

2 Related Work

2.1 Watch Time Prediction

WTP aims to estimate the video watch time based on the user’s profile and video characteristics [27, 28, 41]. Existing techniques fall into three paradigms: (1) *Direct Regression* treats WTP as a point-wise regression task, typically optimized via MSE and often augmented with causal debiasing [11, 40, 42, 43]. However, the underlying Gaussian assumption inevitably leads to mean-collapse. While methods like EGMN [44] attempt to fit mixtures of pre-defined distributions, their performance remains bounded by restrictive parametric assumptions. (2) *Ordinal Regression* [1, 21, 29, 33, 36] transforms the continuous regression problem into a classification task by discretizing time into intervals, suffering from the conditional independence assumption between intervals and rigid

predictions due to fixed quantization granularity. (3) *Discrete Generative* [26] adapts the language modeling to reformulate WTP as a sequence generation task by quantizing continuous time into discrete tokens for autoregressive prediction, which is sensitive to heuristic vocabulary design and incurs prohibitive inference latency. Moreover, these methods collectively fail to capture the intrinsic multimodality and heterogeneity of user-item interaction patterns – a core challenge that this paper tries to address by proposing a new *Continuous Generative Paradigm* and the FlowTime framework.

2.2 Generative Recommendation

Generative recommendation aims to model the underlying distribution of user-item interactions to directly generate personalized results. Early solutions predominantly focused on discrete sequence modeling, utilizing RNNs [8] or Transformers [12, 32] for autoregressive next-item prediction. GR [26] pioneered the application of this paradigm to WTP by quantizing continuous time into discrete tokens for stepwise autoregressive decoding. Recently, continuous generative models like VAEs [13, 15] and diffusion models [9, 22] have gained traction for their superior density estimation capabilities, widely employed to generate high-fidelity item or user representations [18, 19, 37]. However, these approaches have focused almost exclusively on item generation or representation augmentation, and their application to WTP remains unexplored.

2.3 Normalizing Flows Modeling

Normalizing Flows (NFs) were introduced to enhance variational inference through sequences of invertible and differentiable transformations, enabling expressive density modeling with exact likelihood computation [30, 31]. As a general framework for high-dimensional density estimation, NFs have driven significant progress in diverse areas, including architectural innovations like RealNVP [4], continuous probability path modeling via flow matching [22], and representation learning [30]. While NFs have recently emerged in recommendation systems for modeling user preferences [20, 23], their potential for WTP remains unexplored. By leveraging their capability to model complex latent manifolds, we first attempt to harness NFs for WTP and introduce a continuous generative paradigm tailored to capture the heterogeneous interaction patterns.

3 Existing Modeling Paradigms Revisited

3.1 Mean Collapse in Conventional Regression

A common approach for continuous value prediction is point-wise regression with mean squared error (MSE),

$$\min_f \mathbb{E}_{\mathbf{x}, y} [\|y - f(\mathbf{x})\|^2]. \quad (1)$$

The optimal solution of this objective is given by the conditional expectation:

$$f^*(\mathbf{x}) = \mathbb{E}_{P_{\text{data}}} [y | \mathbf{x}], \quad (2)$$

which follows from the first-order optimality condition of the MSE objective. Despite being optimal in expectation, the MSE-optimal predictor may collapse to an average that lies in a low-density region when the conditional distribution is multi-modal.

PROPOSITION 1 (MEAN COLLAPSE EFFECT). *Let $\Delta = \min_{i \neq j} |\mu_i - \mu_j|$ denote the minimum separation between any two modes. If the*

modes are well separated, i.e., $\Delta/\sigma \rightarrow \infty$, then the likelihood of the regression solution under the true conditional distribution vanishes:

$$\lim_{\Delta/\sigma \rightarrow \infty} P_{\text{data}}(f^*(\mathbf{x}) | \mathbf{x}) = 0. \quad (3)$$

It shows that point-wise regression collapses to a low-density prediction that fails to reflect the underlying ordinal structure. The formal proof is provided in Appendix A.2.

3.2 Limitations of Ordinal Regression

Ordinal regression methods (e.g., CREAD [33], SWaT [36]) discretize the continuous watch time y into a sequence of ordered binary decisions using predefined thresholds $c_1 < \dots < c_M$, where $\mathbf{B}^m = \mathbb{I}(y > c_m)$, $m = 1, \dots, M$. This transformation encodes y as a length- M binary vector $\mathbf{B} = (\mathbf{B}^1, \dots, \mathbf{B}^M)$, from which the conditional expectation is approximated by discretization:

$$\mathbb{E}(y | \mathbf{x}) \approx \sum_{m=1}^M P(y > c_m | \mathbf{x}) (c_m - c_{m-1}), \quad (4)$$

with $c_0 = 0$. This reformulation reduces continuous regression to multiple binary classification problems, but introduces structural bias due to quantization and the implicit assumption of conditional independence across interval decisions [26].

PROPOSITION 2 (DEPENDENCY ERROR IN DISCRETIZED MODELING). *Let $P_{\text{data}}(\mathbf{B} | \mathbf{x})$ denote the true joint distribution over interval decisions. A naive discretization model assumes independence,*

$$P_{\text{naive}}(\mathbf{B} | \mathbf{x}) = \prod_{m=1}^M P(\mathbf{B}^m | \mathbf{x}). \quad (5)$$

The modeling error decomposes as

$$D_{\text{KL}}(P_{\text{data}} \| P_{\text{naive}}) = \sum_{m=1}^M \mathbb{E}_{\mathbf{B}_i^{< m}} [D_{\text{KL}}^{(m)}], \quad (6)$$

where $D_{\text{KL}}^{(m)}$ denotes the Kullback-Leibler (KL) divergence between the conditional distribution of the m -th interval decision given its history and the marginal distribution that ignores such dependency.

The proof is provided in Appendix A.1.

3.3 Limitations of Discrete Generative Modeling

Autoregressive (AR) models [26] mitigate the dependency issue by adopting a generative formulation over a sequence of *value tokens*, rather than independent bucket decisions. It represents the continuous target y by a sequence $\mathbf{s} = (s^1, \dots, s^T)$ where t indexes the generation step and T denotes the sequence length. The conditional distribution is modeled via the AR factorization $P(\mathbf{s} | \mathbf{x}) = \prod_{t=1}^T P(s^t | \mathbf{x}, s^{< t})$. With a numeric decoding map $\phi(\cdot)$, the regression target and prediction are given by $y = \sum_{t=1}^T \phi(s^t)$ and $\hat{y} = \sum_{t=1}^T \phi(\hat{s}^t)$, where s^t and \hat{s}^t denote the ground-truth and predicted value tokens at step t , respectively. Accordingly, we define the step-wise regression error as $\Delta_t \triangleq \phi(\hat{s}^t) - \phi(s^t)$.

PROPOSITION 3 (ERROR DECOMPOSITION IN TOKENIZED AUTOREGRESSIVE REGRESSION). *Assume that $\phi(s^t), \phi(\hat{s}^t) \in [w_{\min}, w_{\max}]$, where $[w_{\min}, w_{\max}]$ denotes the numeric range induced by the token vocabulary, and that the step-wise bias satisfies $|\mathbb{E}[\Delta_t]| \leq B$ for all t .*

Then, the expected squared error of the AR prediction $\hat{y} \triangleq \sum_{t=1}^T \phi(\hat{s}^t)$ is upper bounded by

$$\mathbb{E}[(\hat{y} - y)^2] \leq T^2 B^2 + T^2 \frac{(w_{\max} - w_{\min})^2}{4}. \quad (7)$$

Since the bias term B , sequence length T , and value range ($w_{\max} - w_{\min}$) all depend on the chosen vocabulary, heuristic discretization imposes an intrinsic limitation on the accuracy of AR models. A formal proof and further analysis is provided in Appendix A.4.

4 Method

4.1 Problem Formulation

Let $\mathcal{D} = \{(\mathbf{u}_i, \mathbf{v}_i, y_i)\}_{i=1}^N$ denote a dataset of N samples, where $\mathbf{u}_i, \mathbf{v}_i \in \mathbb{R}^d$ denote the user and video feature vectors, respectively, where d is the feature dimension. $y_i \in \mathbb{R}^+$ denotes the observed watch time. Each user and item has their historical watch time sequences, denoted as $\mathcal{H}_i^u = \{h_1^u, \dots, h_{L_u}^u\}$ and $\mathcal{H}_i^v = \{h_1^v, \dots, h_{L_v}^v\}$, respectively. Here, L_u and L_v denote the truncated lengths of the historical sequences. WTP aims to learn a deterministic mapping $f: \mathbf{x} \rightarrow \mathbb{R}^+$, where $\mathbf{x} = (\mathbf{u}, \mathbf{v})$, to minimize the discrepancy between the predicted value \hat{y} and ground truth y .

Departing from the traditional point estimation paradigm, we reformulate WTP as a continuous generative modeling problem. Our goal is to learn the true underlying conditional probability density $p_{\text{data}}(y | \mathbf{x})$, where y is treated as a continuous random variable. This objective is achieved by maximizing the marginal likelihood of the observed watch time y conditioned on \mathbf{x} :

$$p_{\theta}(y | \mathbf{x}) = \int_{\mathbf{z}} p_{\theta}(y | \mathbf{z}, \mathbf{x}) p_{\psi}(\mathbf{z} | \mathbf{x}) dz, \quad (8)$$

where $\mathbf{z} \in \mathbb{R}^d$ denotes a latent variable, θ parameterizes the conditional likelihood (decoder), and ψ parameterizes the conditional prior over the latent space. In essence, this formulation allows the framework to model the multimodality and heterogeneity prevalent in real-world continuous watch time distributions.

4.2 Overall Architecture of FlowTime

As illustrated in Fig. 3, FlowTime is built upon a VAE backbone, designed for efficient one-step continuous generative regression. The framework comprises two principal components: a Probabilistic Encoder that approximates the posterior distribution of the latent variables given the target and user/video features, and a Generative Decoder that reconstructs the watch time distribution from the latent space.

4.2.1 Probabilistic Encoder. The encoder approximates the intractable true posterior of the latent variable by conditioning the prior $p_{\psi}(\mathbf{z} | \mathbf{x})$ on the observed watch time. Formally, given the static features $\mathbf{x}_i = (\mathbf{u}_i, \mathbf{v}_i)$ and the target y_i , the encoder models the approximate posterior distribution $q_{\phi}(\mathbf{z} | y_i, \mathbf{x}_i)$ as a multivariate Gaussian:

$$q_{\phi}(\mathbf{z} | y_i, \mathbf{x}_i) = \mathcal{N}(\mathbf{z}; \mu_{\phi}(y_i, \mathbf{x}_i), \sigma_{\phi}^2(y_i, \mathbf{x}_i)\mathbf{I}), \quad (9)$$

where $\mu_{\phi}(\cdot)$ and $\sigma_{\phi}(\cdot)$ are Multi-Layer Perceptrons (MLPs) that predict the mean and diagonal covariance of the latent variable $\mathbf{z} \in \mathbb{R}^d$. To enable backpropagation through the stochastic sampling process, we employ the reparameterization trick [14]. Specifically,

the latent variable \mathbf{z} is sampled as:

$$\mathbf{z} = \mu_{\phi}(y_i, \mathbf{x}_i) + \sigma_{\phi}(y_i, \mathbf{x}_i) \odot \epsilon, \quad \text{where } \epsilon \sim \mathcal{N}(\mathbf{0}, \mathbf{I}), \quad (10)$$

where \odot denotes the element-wise product. This transformation decouples the stochastic noise ϵ from the network parameters, allowing for end-to-end optimization.

4.2.2 Generative Decoder. The decoder functions as the generative network, aiming to reconstruct the target watch time y_i from the sampled latent variable \mathbf{z} , conditioned on the static features \mathbf{x}_i . We model the likelihood distribution $p_{\theta}(y_i | \mathbf{z}, \mathbf{x}_i)$ as:

$$p_{\theta}(y_i | \mathbf{z}, \mathbf{x}_i) = \mathcal{N}(y_i; \mu_{\theta}(\mathbf{z}, \mathbf{x}_i), \sigma_{\theta}^2(\mathbf{z}, \mathbf{x}_i)), \quad (11)$$

where μ_{θ} and σ_{θ} are MLP-based networks mapping the latent feature space back to the target space. Following the standard VAE formulation, during training the latent variable is sampled from the approximate posterior $\mathbf{z} \sim q_{\phi}(\mathbf{z} | y_i, \mathbf{x}_i)$, which enables reconstruction-based learning of the generative model. During inference, the latent variable is instead sampled from the conditional prior $\mathbf{z} \sim p_{\psi}(\mathbf{z} | \mathbf{x}_i)$. For efficient deterministic prediction, we often simplify this to predicting the mean expectation $\hat{y}_i = \mu_{\theta}(\mathbf{z}, \mathbf{x}_i)$.

4.2.3 Optimization Objective. The model is trained by maximizing the Evidence Lower Bound (ELBO) of the log-likelihood, and the objective is formulated as:

$$\mathcal{L}_{\text{VAE}} = \mathbb{E}_{q_{\phi}(\mathbf{z} | y_i, \mathbf{x}_i)} [\log p_{\theta}(y_i | \mathbf{z}, \mathbf{x}_i)] - \text{KL}(q_{\phi}(\mathbf{z} | y_i, \mathbf{x}_i) \| p_{\psi}(\mathbf{z} | \mathbf{x}_i)), \quad (12)$$

where the first term represents the reconstruction loss by Mean Squared Error for Gaussian likelihoods, and the second term is the KL divergence regularizing the posterior towards a prior distribution $p_{\psi}(\mathbf{z} | \mathbf{x}_i)$.

However, in standard VAE, the prior $p_{\psi}(\mathbf{z} | \mathbf{x}_i)$ is typically assumed to be a standard isotropic Gaussian, i.e., $p(\mathbf{z} | \mathbf{x}_i) \sim \mathcal{N}(\mathbf{0}, \mathbf{I})$. While this assumption simplifies the KL computation, it imposes a strong topological constraint, forcing the latent space to be unimodal and globally shared across all users. However, a static, user-agnostic Gaussian prior is fundamentally ill-suited for such distributional heterogeneity, often leading to over-smoothed predictions or 'posterior collapse'. To address this, we introduce a Flow-based Personalized Prior, which replaces the static $p(\mathbf{z} | \mathbf{x}_i)$ by explicitly conditioning the latent density on historical interaction patterns.

4.3 Flow-based Personalized Prior

To transcend the expressivity limitations of the isotropic Gaussian prior inherent in standard VAEs, we propose a Flow-based Personalized Prior. This module leverages NFs to construct a complex, multimodal prior distribution $p(\mathbf{z} | \mathbf{x}_i)$ explicitly conditioned on historical interaction patterns. By learning a sequence of invertible transformations driven by user and item histories, the model adaptively warps a simple base density into a structured, pattern-specific latent manifold.

4.3.1 Pattern Encoding. First, to capture the distributional characteristics of historical interactions, we represent the watch time histories of the user (\mathcal{H}_i^u) and the item (\mathcal{H}_i^v) via their quantile statistics. Let $\mathbf{q}^u = \{q_1^u, \dots, q_L^u\}$ and $\mathbf{q}^v = \{q_1^v, \dots, q_L^v\}$ denote the sequences of L quantiles extracted from \mathcal{H}_i^u and \mathcal{H}_i^v , respectively. These quantile-based representations encode the global shape of

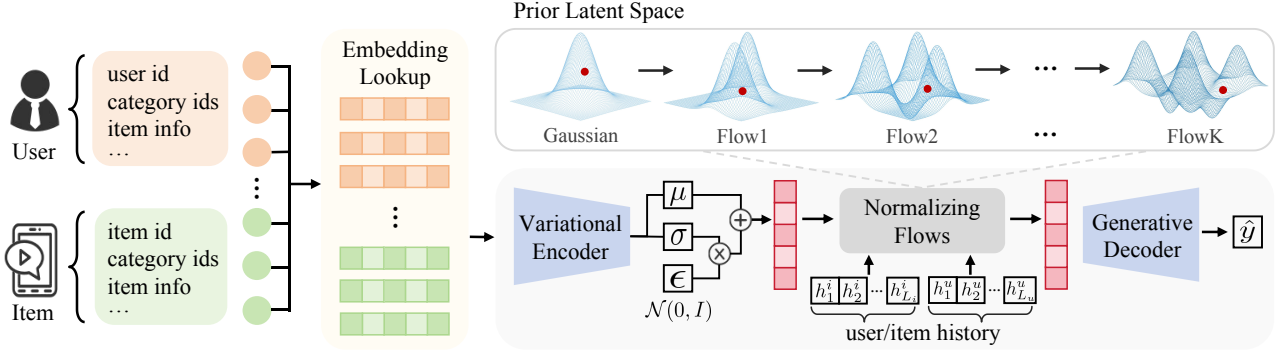


Figure 3: The overall architecture of FlowTime. The framework employs a Variational Encoder to map inputs into a stochastic latent space. Crucially, we introduce a Flow-based Personalized Prior, which leverages Normalizing Flow conditioned on user/item interaction histories to progressively warp a standard Gaussian into a complex, pattern-specific latent manifold, enabling the Generative Decoder to yield precise watch time predictions.

historical watch-time distributions. Together with the static user and item features, they form the contextual condition used for prediction, which we define as $\mathbf{c} = [\mathbf{q}^u, \mathbf{q}^v]$ as the condition for prediction. These ordered sequences provide a compact yet robust summary of long-term viewing patterns. We employ a Transformer-based architecture to encode these quantile sequences into dense contextual embeddings. Specifically, the quantiles are projected and augmented with positional encodings to preserve their ordinal structure:

$$\mathbf{E}^u = \text{Transformer}(\text{Proj}(\mathbf{q}^u) + \mathbf{P}), \mathbf{E}^v = \text{Transformer}(\text{Proj}(\mathbf{q}^v) + \mathbf{P}), \quad (13)$$

where \mathbf{P} denotes the positional embeddings. The self-attention mechanism aggregates distributional patterns across the input sequence, followed by mean pooling: $\mathbf{h}^u = \text{MeanPool}(\mathbf{E}^u)$, $\mathbf{h}^v = \text{MeanPool}(\mathbf{E}^v)$. The final conditioning context $\mathbf{h}_{\text{prior}}$ is obtained by concatenating these representations:

$$\mathbf{h}_{\text{prior}} = [\mathbf{h}^u \parallel \mathbf{h}^v] \in \mathbb{R}^{2d}. \quad (14)$$

4.3.2 Manifold Warping via Conditional NFs. Given the context $\mathbf{h}_{\text{prior}}$, we construct the personalized prior distribution by transforming a simple base distribution \mathbf{z}^0 inferred by \mathbf{z} through a sequence of K invertible mappings. Formally, let $f_k : \mathbb{R}^d \mapsto \mathbb{R}^d$ be a bijective function parameterized by ψ_k and conditioned on $\mathbf{h}_{\text{prior}}$. The transformation chain is defined as:

$$\mathbf{z}^k = f_k(\mathbf{z}^{k-1}; \mathbf{h}_{\text{prior}}), \quad k = 1, \dots, K, \quad (15)$$

where \mathbf{z}^K represents the final latent variable sampled from the complex prior. In this work, we instantiate f_k using Conditional Planar Flows, which offer an efficient mechanism for non-linear expansion and contraction of the density:

$$\mathbf{z}^k = \mathbf{z}^{k-1} + \mathbf{u}_k(\mathbf{h}_{\text{prior}}) \cdot \tanh\left(\mathbf{w}_k(\mathbf{h}_{\text{prior}})^\top \mathbf{z}^{k-1} + b_k(\mathbf{h}_{\text{prior}})\right), \quad (16)$$

where the parameters $\mathbf{u}_k, \mathbf{w}_k, b_k$ are dynamically generated from $\mathbf{h}_{\text{prior}}$ via MLPs. According to the change of variables theorem [31],

the log-density of the transformed latent variable \mathbf{z} under the personalized prior $p_\psi(\mathbf{z}^k | \mathbf{c})$ can be computed exactly as:

$$\log p_\psi(\mathbf{z}^k | \mathbf{c}) = \log p_0(\mathbf{z}^0) - \sum_{k=1}^K \log \det \left| \frac{\partial f_k(\mathbf{z}^{k-1}; \mathbf{h}_{\text{prior}})}{\partial \mathbf{z}^{k-1}} \right|. \quad (17)$$

This formulation allows the model to adaptively warp the isotropic Gaussian \mathbf{z}^0 into a complex, user-item pattern-specific manifold. Conditioned on the transformed latent variable \mathbf{z}^K and the input features \mathbf{x} , the decoder produces the estimation of watch time via

$$\hat{y} = \mu_\theta(\mathbf{z}^K, \mathbf{x}), \quad (18)$$

thereby enabling distribution-aware continuous regression.

4.4 Joint Optimization Objectives

To jointly improve prediction accuracy and distributional fidelity, we design a multi-objective loss.

Accuracy Anchoring. In the observation space, we adopt the Huber loss $\mathcal{L}_{\text{Huber}}$ [10], which serves as an accuracy anchor that directly constrains point estimates and improves regression fidelity:

$$\mathcal{L}_{\text{base}} = \mathcal{L}_{\text{Huber}}(y, \hat{y}) = \mathcal{L}_{\text{Huber}}(y, \mu_\theta(\mathbf{z}^K, \mathbf{x})). \quad (19)$$

Latent Space Regularization. In the latent space, we align the approximate posterior $q_\phi(\mathbf{z}^0 | y, \mathbf{c})$ with a standard Gaussian distribution via KL divergence:

$$\mathcal{L}_{\text{latent}} = \text{KL}(q_\phi(\mathbf{z}^0 | y, \mathbf{c}) \parallel \mathcal{N}(\mathbf{0}, \mathbf{I})) \quad (20)$$

This loss preserves continuity and identifiability in the latent space.

Distribution Alignment. To align the generated watch-time distribution with historical interaction patterns, we introduce a Wasserstein distance-based loss on quantile representations. Specifically, we generate the samples $\hat{y}^l = \mu_\theta(\mathbf{z}_l^K, \mathbf{x})$ with latent vectors \mathbf{z}_l^K sampled from the NF-based prior. Using the user and item side quantiles \mathbf{q}^u and \mathbf{q}^v defined above, we align the order statistics of these generated samples via the following joint objective:

$$\mathcal{L}_{\text{W-Dist}} = \frac{1}{L} \sum_{l=1}^L \left(\lambda \left| \hat{y}^{(l)} - q_l^u \right| + (1 - \lambda) \left| \hat{y}^{(l)} - q_l^v \right| \right), \quad (21)$$

Table 1: Statistics of the datasets used in our TimeRec Library.

| Dataset | # Users | # Items | # Impressions | Characteristics |
|---------------|---------|---------|---------------|-----------------|
| KuaiRand-Pure | 27,285 | 7,583 | 1,186,059 | Unbiased |
| KuaiRec | 7,176 | 10,728 | 12,530,806 | High Density |

where λ balances the influence of user and item level distributional alignment.

Finally, the whole training objective is as follows:

$$\mathcal{L} = \lambda_1 \mathcal{L}_{\text{base}} + \lambda_2 \mathcal{L}_{\text{latent}} + \mathcal{L}_{\text{W-Dist}}. \quad (22)$$

4.5 Capturing Multimodality via Generative Modeling

FlowTime adopts a continuous generative regression paradigm that directly models conditional distributions in continuous spaces. Assume that under optimization, $\mu_\theta(\mathbf{z})$ aligns with a finite set of dominant conditional modes $\{\alpha_k\}_{k=1}^K \subset \mathbb{R}$ of the true conditional distribution $p_{\text{data}}(y | x)$. We define the latent region associated with mode k as $\mathcal{Z}_k = \{\mathbf{z} \mid \|\mu_\theta(\mathbf{z}) - \alpha_k\| \leq \varepsilon\}$.

PROPOSITION 4 (LATENT SPACE PARTITIONING). *Assume that $\mu_\theta(\cdot)$ is L -Lipschitz continuous and let $\Delta \triangleq \min_{i \neq j} \|\alpha_i - \alpha_j\|$ denote the minimum separation between distinct conditional modes. If $\Delta > 2\varepsilon$, then the latent regions $\{\mathcal{Z}_k\}$ are pairwise disjoint and satisfy*

$$\mathcal{Z}_i \cap \mathcal{Z}_j = \emptyset, \quad \|\mathbf{z}_i - \mathbf{z}_j\| \geq \frac{\Delta - 2\varepsilon}{L}, \quad \forall \mathbf{z}_i \in \mathcal{Z}_i, \mathbf{z}_j \in \mathcal{Z}_j, i \neq j. \quad (23)$$

$$\mathbf{z} \in \mathcal{Z}_k \implies \|\mu_\theta(\mathbf{z}) - \alpha_k\| \leq \varepsilon, \quad (24)$$

i.e., each latent region decodes to a distinct high-density conditional mode, thereby avoiding collapse to low-density averages.

The formal proof and its probabilistic extension under NF-based sampling are provided in Appendix A.3.

5 Experiments

This section presents extensive experiments to demonstrate the effectiveness of FlowTime. Five research questions are explored:

- **RQ1:** Does FlowTime outperform state-of-the-art baselines in both offline accuracy and online commercial metrics?
- **RQ2:** How is FlowTime compared to other paradigms in terms of computational efficiency versus predictive accuracy?
- **RQ3:** How effective is each major module in FlowTime?
- **RQ4:** Does FlowTime mitigate the ‘‘mean-collapse’’ issue and capture fine-grained user-item interaction patterns?
- **RQ5:** How sensitive is FlowTime to key hyperparameters?

5.1 The TimeRec Library

To address the prevalence of inconsistent evaluation and foster reproducible research, we develop TimeRec, the first open-source unified benchmarking library for the watch time prediction domain. TimeRec standardizes the entire experimental pipeline by integrating diverse datasets, rigorous feature engineering, and reproduced SOTA methods to ensure fair and consistent comparisons.

5.1.1 Datasets. We evaluate all methods on two public datasets and one industrial dataset, with statistics summarized in Tab. 1.

- (1) **KuaiRand-Pure** [6]. Derived from Kuaishou’s random dispatching policy, this dataset provides unbiased interaction data free from system-induced selection biases, making it ideal for validating intrinsic user interest modeling.
- (2) **KuaiRec** [5]: A fully observed dataset characterized by high density. The rich user-item interactions facilitate precise evaluation of fine-grained patterns and long-term user habits.
- (3) **Indust:** A large-scale industrial dataset sourced from a short-video platform with over 400 million DAUs and multi-billion impressions each day. It exhibits extreme sparsity and long-tail distributions, reflecting real-world deployment challenges.

5.1.2 Feature Engineering.

Data Splitting. We implement a rigorous time-based splitting strategy for Indust, which utilizes interaction logs from 5 consecutive days for training and the subsequent day for testing. KuaiRand and KuaiRec strictly adhere to their standard chronological train/test splits provided by the original work [5, 6].

Feature Sets. Following [39], we align feature configurations for public datasets. Both utilize ‘user_id’ and ‘onehot_feat0~17’ as user features. Item features comprise ‘item_id’, ‘duration’, and dataset-specific attributes: ‘feat0~4’ for KuaiRec and ‘feat0~3’ for KuaiRand.

5.1.3 Baselines. We reproduce representative SOTA methods for rigorous evaluation, categorized into three established paradigms:

- **Direct Regression** [40, 42–44]: MSE-based models, including variants augmented with causal debiasing or multi-Gaussian fitting.
- **Ordinal Regression** [1, 21, 33, 36] Methods that discretize continuous time into intervals for classification.
- **Discrete Generative Regression** [26]: Approaches utilizing language modeling to generate quantized time tokens.

Differently, our FlowTime represents a novel (or the fourth) paradigm – **Continuous Generative Regression**.

5.1.4 Evaluation Protocols. We employ two standard metrics and a novel personalization fidelity metric to comprehensively evaluate predictive performance:

- **Mean Average Error (MAE):** Quantifies point-wise regression accuracy between predicted values $\{\hat{y}_i\}_{i=1}^N$ and actual values $\{y_i\}_{i=1}^N$, denoted as $\frac{1}{N} \sum_{i=1}^N |\hat{y}_i - y_i|$.
- **XAUC** [40]: For all valid pairs $\mathcal{P} = \{(i, j) \mid y_i > y_j\}$, XAUC is defined as the proportion of correctly ordered predictions, denoted as $\frac{1}{|\mathcal{P}|} \sum_{(i,j) \in \mathcal{P}} \mathbb{I}(\hat{y}_i > \hat{y}_j)$, where $\mathbb{I}(\cdot)$ is the indicator function. A higher XAUC indicates superior ranking capability.
- **Personalized Distributional Fidelity (PDF):** To evaluate personalized pattern capture, we introduce PDF, defined as the average Jensen-Shannon Divergence between the histogram-binned probability distributions of ground-truth P_u and predicted Q_u watch time sequences for each user:

$$\text{PDF-U} = \mathbb{E}_u \left[\frac{1}{2} \text{KL}(P_u \parallel M_u) + \frac{1}{2} \text{KL}(Q_u \parallel M_u) \right] \quad (25)$$

where $M_u = \frac{1}{2}(P_u + Q_u)$. We report both User-level (PDF-U) and Item-level (PDF-I) scores.

Table 2: Performance comparison among different approaches on KuaiRec, KuaiRand, and the Indust dataset. For comparative clarity, FlowTime is grouped under “Generative Regression” here.

| Paradigm | Method | KuaiRec | | | | KuaiRand | | | | Indust | |
|-----------------------|--------------------------------|---------------|---------------|---------------|---------------|----------------|---------------|---------------|---------------|----------------|---------------|
| | | MAE ↓ | XAUC ↑ | PDF-U ↓ | PDF-I ↓ | MAE ↓ | XAUC ↑ | PDF-U ↓ | PDF-I ↓ | MAE ↓ | XAUC ↑ |
| Direct Regression | VR (<i>value regression</i>) | 3.3973 | 0.5822 | 0.3073 | 0.1232 | 22.1504 | 0.6429 | 0.7386 | 0.7363 | 21.3199 | 0.6041 |
| | D2Q [40] (<i>KDD'22</i>) | 3.2696 | 0.6043 | 0.3210 | 0.1798 | 19.4258 | <u>0.6715</u> | 0.6697 | 0.5665 | 19.6098 | 0.6156 |
| | D2Co [43] (<i>Recsys'23</i>) | 3.2633 | 0.5895 | 0.3055 | 0.1346 | 20.7854 | 0.6547 | 0.7435 | 0.6333 | 20.3233 | 0.6053 |
| | CWM [42] (<i>KDD'24</i>) | 3.3532 | 0.5899 | 0.3010 | 0.1521 | 19.6351 | 0.6668 | <u>0.6289</u> | 0.5908 | 19.9865 | 0.6085 |
| | EGMN [44] (<i>Recsys'25</i>) | <u>3.1803</u> | <u>0.6125</u> | 0.2646 | 0.0874 | 19.3246 | 0.6682 | 0.6503 | <u>0.5414</u> | 18.2354 | 0.6155 |
| | DIFL [11] (<i>AAAI'26</i>) | 3.2420 | 0.6055 | 0.3103 | 0.1544 | 19.3181 | 0.6708 | 0.6529 | 0.5374 | 17.5606 | 0.6188 |
| Ordinal Regression | TPM [21] (<i>KDD'23</i>) | 3.4584 | 0.5819 | 0.2844 | 0.1238 | 22.5950 | 0.6303 | 0.7567 | 0.7770 | 19.2344 | 0.6055 |
| | CREAD [33] (<i>AAAI'24</i>) | 3.2290 | 0.6123 | 0.2741 | 0.1053 | 19.8087 | 0.6678 | 0.7028 | 0.6479 | 17.9823 | 0.6134 |
| | PTPM [1] (<i>CIKM'25</i>) | 3.2865 | 0.6033 | 0.2787 | 0.1169 | 20.6584 | 0.6679 | 0.7345 | 0.6993 | 18.4263 | 0.6111 |
| | SWaT [36] (<i>KDD'25</i>) | 3.3496 | 0.5888 | 0.3308 | 0.1168 | 22.3353 | 0.6515 | 0.7456 | 0.7303 | 20.4522 | 0.6098 |
| Generative Regression | GR [26] (<i>WWW'26</i>) | 3.1985 | 0.6124 | <u>0.2644</u> | <u>0.0833</u> | <u>19.2742</u> | 0.6682 | 0.6664 | 0.6570 | <u>17.2503</u> | <u>0.6201</u> |
| | FlowTime (Ours) | 3.1588 | 0.6174 | 0.2634 | 0.0823 | 19.1045 | 0.6751 | 0.5974 | 0.4861 | 16.9553 | 0.6243 |

The best and second best results are marked in **bold** and underline, respectively. ↑ indicates that higher values are better, while ↓ indicates the opposite. Each experiment is repeated 5 times and the average is reported.

Table 3: Performance gain on online A/B testing.

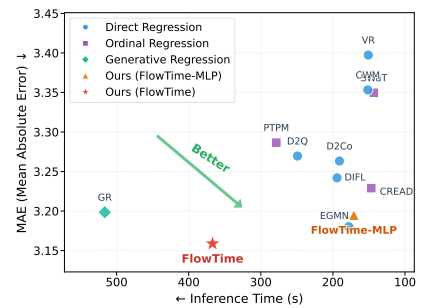
| Metric | Uplift | P-value | 95% CI |
|-----------------|---------|---------|----------------|
| APP Usage Time | +1.027% | 0.003 | [0.82%, 1.23%] |
| Video Play Time | +1.044% | 0.001 | [0.91%, 1.18%] |
| Long-view Rate | +0.892% | 0.002 | [0.65%, 1.13%] |
| Share Rate | +1.236% | 0.005 | [0.95%, 1.52%] |

5.1.5 Implementation Details. All models are trained for 20 epochs using the Adam optimizer ($\beta_1 = 0.9$, $\beta_2 = 0.999$) with a batch size of 1024 and learning rate of $5e^{-4}$. To ensure fair comparison, we adopt the optimal hyperparameters reported in the original papers for all baselines. Furthermore, for shared modules across different models (e.g. feature encoders), we strictly align the number of parameters to ensure that performance gains are derived from method superiority rather than model capacity.

5.2 Performance Comparison (RQ1)

5.2.1 Offline Evaluation. Table 2 reports the comparative results across three datasets, where FlowTime consistently establishes a new state-of-the-art across all metrics. First, compared to Direct Regression baselines, FlowTime effectively mitigates the “mean-collapse” issue inherent in MSE-based optimization. This is evidenced by a substantial reduction in MAE by 0.676% and an XAUC lift of 0.8% on the KuaiRec dataset. Second, against Ordinal and Discrete Generative paradigms, FlowTime achieves superior precision by avoiding quantization errors. This advantage is manifested as a 0.704 MAE reduction on KuaiRand, and simultaneous improvements on Indust (MAE 1.027, XAUC 1.777%). Most notably, FlowTime demonstrates superior flexibility and effectiveness over the mixture-density-based EGMN, reducing PDF-U and PDF-I by 0.454% and 5.835% on KuaiRec, respectively. This demonstrates the superior expressivity of our flow-based architecture in modeling complex interaction patterns.

5.2.2 Online A/B Testing. To validate real-world efficacy, we deploy FlowTime in the Trending Video Recommendation scenario of a

**Figure 4: The efficiency-performance trade-off comparison of FlowTime against baselines. The bottom-right corner represents lower error and faster inference.**

leading platform with over 400 million DAUs. Serving 10% of traffic for six days, FlowTime achieves statistically significant gains across all core metrics, as detailed in Table 3 with corresponding P-values and 95% Confidence Intervals (CI). Specifically, it yields substantial commercial value with a **1.044%** uplift in Video Play Time and **1.027%** in App Usage Time. Crucially, it also significantly boosts interaction metrics (e.g., **+1.236%** Share Rate), effectively enhancing recommendation accuracy and user satisfaction.

5.3 Efficiency-Performance Analysis (RQ2)

Fig. 4 visualizes the trade-off between inference speed and prediction accuracy across paradigms, where FlowTime achieves a superior balance. While marginally slower than direct regression models, it offers significantly higher accuracy. Furthermore, the FlowTime-MLP variant (ablated in Table 4) further accelerates inference, closing the speed gap. Crucially, compared to the generative baseline GR, FlowTime realizes a twofold improvement: it enhances accuracy while markedly reducing inference latency by nearly **30%**. This substantiates the dual superiority of our one-step continuous generative architecture and Flow-based Personalized Priors in

Table 4: Ablation study on generative architectures, normalizing flow components, and history modeling strategies.

| Variant | MAE | XAUC | PDF-U | PDF-I |
|--------------------------------|--------------|--------------|--------------|--------------|
| (a) FlowTime (Ours) | 3.159 | 0.617 | 0.249 | 0.078 |
| <i>Generative Architecture</i> | | | | |
| (b) w/ DDPM [9] | 3.163 | 0.613 | 0.251 | 0.081 |
| (c) w/ Flow Matching [22] | 3.161 | 0.614 | 0.250 | 0.080 |
| <i>Distribution Modeling</i> | | | | |
| (d) w/o Normalizing Flows | 3.245 | 0.607 | 0.304 | 0.113 |
| <i>History Modeling</i> | | | | |
| (e) w/o User History | 3.281 | 0.599 | 0.303 | 0.081 |
| (f) w/o Item History | 3.235 | 0.605 | 0.253 | 0.111 |
| (g) w/o Both & NF | 3.318 | 0.593 | 0.308 | 0.127 |
| (h) Rep. Trans. w/ MLP | 3.195 | 0.611 | 0.251 | 0.081 |

terms of both efficiency and effectiveness, particularly over iterative autoregressive mechanisms.

5.4 Ablation Study (RQ3)

We validate the efficacy of FlowTime’s core components across three dimensions as shown in Tab. 4.

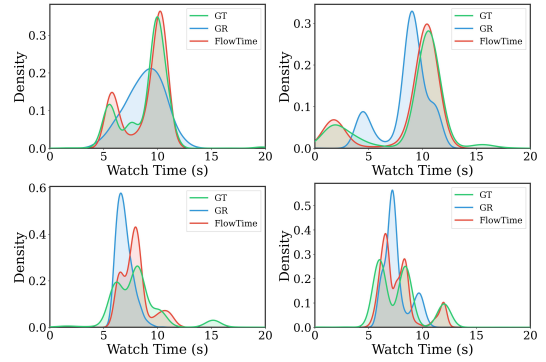
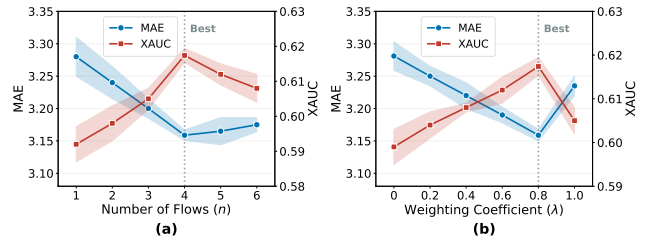
Impact of Generative Architecture. The mainstream iterative baselines such as Diffusion [9] and Flow Matching [22] outperform SOTA methods, confirming the efficacy of continuous generative modeling. Nevertheless, FlowTime consistently achieves the best results (Row (a) vs. Rows (b-c)). This superiority suggests that our one-step approach offers a robust inductive bias for high-sparsity scenarios, effectively circumventing the error accumulation inherent in iterative denoising while ensuring low latency.

Necessity of NFs. Reverting the Flow-based prior to a standard Gaussian (VAE) degrades MAE by 2.72% and XAUC by 1.62% (Row (a) vs. Row (d)). This sharp drop verifies that static priors fail to capture the multimodality of watch time, underscoring the criticality of NFs in modeling complex preference distributions.

Effectiveness of History Modeling. (1) Removing both user and item histories (Row (g)) yields the worst performance, confirming the pivotal role of historical interaction patterns in personalization. (2) User history proves more critical than item history, indicating user habits are the primary drivers (Row (e) vs. Row (f)). (3) Replacing the Transformer with an MLP (Row (h)) degrades XAUC by ~1%, highlighting the necessity of attention mechanisms for capturing global behavioral patterns.

5.5 The Analysis of Personalized Patterns (RQ4)

5.5.1 Prediction Distributions Analysis. We visualize the predicted watch time distributions for representative user-item pairs to assess the model’s capability in capturing complex interaction patterns. > As shown in Fig. 5, compared to GR, FlowTime exhibits superior distributional fidelity, accurately reconstructing the Ground Truth (GT) distributions across diverse shapes, including bimodal and trimodal. This confirms that by modeling the latent manifold via NFs, our framework effectively captures personalized user-item interaction patterns.

**Figure 5: Visualization of distributional fidelity.****Figure 6: Ablation study on key hyperparameters. (a) Impact of the number of flow steps (n) on model performance. (b) Impact of the user-item weighting coefficient (λ).**

5.6 Effect of Hyperparameters (RQ5)

We investigate the impact of two critical hyperparameters: the number of flow steps K (in Eq. 15) and the user-item weighting coefficient λ (in Eq. 21). Fig. 6 illustrates the results on the KuaiRec dataset. K controls the complexity of the bijective transformation. As shown Fig. 6(a), performance improves consistently as K increases, peaking at $K = 4$, before exhibiting a slight decline. This suggests that while sufficient flow depth is necessary to model complex manifold topologies, an excessive number of steps may induce overfitting or optimization difficulties.

This coefficient λ modulates the trade-off between user and item patterns in constructing the prior latent space. As λ increases, performance steadily improves, corroborating our finding that user-specific patterns are the primary determinants of watch time. However, performance degrades beyond $\lambda = 0.8$. This inflection point indicates that while user patterns are dominant, item-specific patterns remain indispensable for precise WTP, and neglecting them undermines model fidelity.

6 Conclusion

This paper addresses the intrinsic heterogeneity of watch time distributions by proposing **FlowTime**, a novel framework under the *Continuous Generative Regression* paradigm. Through the causal modeling of interaction patterns and the design of a Flow-based Personalized Prior, FlowTime effectively captures multimodal user-item interaction patterns while ensuring real-time inference. Our work not only sets a new SOTA but also bridges the gap in standardized evaluation by constructing the *TimeRec* library, paving the way for more fair and consistent benchmarking in future research.

Acknowledgments. This work was partially supported by Kuaishou Technology. Jihong Guan was supported by the National Social Science Fund of China (NSFC) under grant No. 24&ZD185. The computations in this research were performed using the CFFF platform of Fudan University.

References

- [1] Xiaokai Chen, Xiao Lin, Changcheng Li, and Peng Jiang. 2025. Personalized Tree-Based Progressive Regression Model for Watch-Time Prediction in Short Video Recommendation. In *Proceedings of the 34th ACM International Conference on Information and Knowledge Management*. 5609–5616.
- [2] Paul Covington, Jay Adams, and Emre Sargin. 2016. Deep neural networks for youtube recommendations. In *Proceedings of the 10th ACM conference on recommender systems*. 191–198.
- [3] James Davidson, Benjamin Liebald, Junning Liu, Palash Nandy, Taylor Van Vleet, Ullas Gargi, Sujoy Gupta, Yu He, Mike Lambert, Blake Livingston, et al. 2010. The YouTube video recommendation system. In *Proceedings of the fourth ACM conference on Recommender systems*. 293–296.
- [4] Laurent Dinh, Jascha Sohl-Dickstein, and Samy Bengio. 2017. Density estimation using Real NVP. In *International Conference on Learning Representations*. <https://openreview.net/forum?id=HkpbH9lx>
- [5] Chongming Gao, Shijun Li, Wenqiang Lei, Jiawei Chen, Biao Li, Peng Jiang, Xiangnan He, Jiabin Mao, and Tat-Seng Chua. 2022. KuaiRec: A fully-observed dataset and insights for evaluating recommender systems. In *Proceedings of the 31st ACM International Conference on Information & Knowledge Management*. 540–550.
- [6] Chongming Gao, Shijun Li, Yuan Zhang, Jiawei Chen, Biao Li, Wenqiang Lei, Peng Jiang, and Xiangnan He. 2022. Kuairand: An unbiased sequential recommendation dataset with randomly exposed videos. In *Proceedings of the 31st ACM international conference on information & knowledge management*. 3953–3957.
- [7] Xudong Gong, Qinlin Feng, Yuan Zhang, Jiangling Qin, Weijie Ding, Biao Li, Peng Jiang, and Kun Gai. 2022. Real-time short video recommendation on mobile devices. In *Proceedings of the 31st ACM international conference on information & knowledge management*. 3103–3112.
- [8] Balázs Hidasi, Alexandros Karatzoglou, Linas Baltrunas, and Domonkos Tikk. 2015. Session-based recommendations with recurrent neural networks. *arXiv preprint arXiv:1511.06939* (2015).
- [9] Jonathan Ho, Ajay Jain, and Pieter Abbeel. 2020. Denoising diffusion probabilistic models. *Advances in neural information processing systems* 33 (2020), 6840–6851.
- [10] Peter J Huber. 1992. Robust estimation of a location parameter. In *Breakthroughs in statistics: Methodology and distribution*. Springer, 492–518.
- [11] Chenghou Jin, Yixin Ren, Hongxu Ma, Yewei Xia, Yi Guan, Hao Zhang, Jiandong Ding, Jihong Guan, and Shuigeng Zhou. 2026. Invariant Feature Learning for Counterfactual Watch-time Prediction in Video Recommendation. In *Proceedings of the AAAI Conference on Artificial Intelligence*, Vol. 40. 14964–14972.
- [12] Wang-Cheng Kang and Julian McAuley. 2018. Self-attentive sequential recommendation. In *2018 IEEE international conference on data mining (ICDM)*. IEEE, 197–206.
- [13] Diederik P Kingma and Max Welling. 2013. Auto-encoding variational bayes. *arXiv preprint arXiv:1312.6114* (2013).
- [14] Diederik P Kingma and Max Welling. 2013. Auto-encoding variational bayes. *arXiv preprint arXiv:1312.6114* (2013).
- [15] Diederik P Kingma, Max Welling, et al. 2019. An introduction to variational autoencoders. *Foundations and Trends® in Machine Learning* 12, 4 (2019), 307–392.
- [16] Qizhen Lan, Yu-Chun Hsu, Nida Saddaf Khan, and Xiaoqian Jiang. 2026. ReCo-KD: Region-and Context-Aware Knowledge Distillation for Efficient 3D Medical Image Segmentation. *arXiv preprint arXiv:2601.08301* (2026).
- [17] Qizhen Lan and Qing Tian. 2025. ACAM-KD: adaptive and cooperative attention masking for knowledge distillation. In *Proceedings of the IEEE/CVF International Conference on Computer Vision*. 3957–3966.
- [18] Wuchao Li, Rui Huang, Haijun Zhao, Chi Liu, Kai Zheng, Qi Liu, Na Mou, Guorui Zhou, Defu Lian, Yang Song, et al. 2025. DimeRec: a unified framework for enhanced sequential recommendation via generative diffusion models. In *Proceedings of the Eighteenth ACM International Conference on Web Search and Data Mining*. 726–734.
- [19] Zihao Li, Aixin Sun, and Chenliang Li. 2023. Diffurec: A diffusion model for sequential recommendation. *ACM Transactions on Information Systems* 42, 3 (2023), 1–28.
- [20] Dawen Liang, Rahul G Krishnan, Matthew D Hoffman, and Tony Jebara. 2018. Variational autoencoders for collaborative filtering. In *Proceedings of the 2018 world wide web conference*. 689–698.
- [21] Xiao Lin, Xiaokai Chen, Linfeng Song, Jingwei Liu, Biao Li, and Peng Jiang. 2023. Tree based progressive regression model for watch-time prediction in short-video recommendation. In *Proceedings of the 29th ACM SIGKDD Conference on Knowledge Discovery and Data Mining*. 4497–4506.
- [22] Yaron Lipman, Ricky TQ Chen, Heli Ben-Hamu, Maximilian Nickel, and Matt Le. 2022. Flow matching for generative modeling. *arXiv preprint arXiv:2210.02747* (2022).
- [23] Feng Liu, Lixin Zou, Xiangyu Zhao, Min Tang, Liming Dong, Dan Luo, Xiangyang Luo, and Chenliang Li. 2025. Flow Matching based Sequential Recommender Model. *arXiv preprint arXiv:2505.16298* (2025).
- [24] Shang Liu, Zhenzhong Chen, Hongyi Liu, and Xinghai Hu. 2019. User-video co-attention network for personalized micro-video recommendation. In *The world wide web conference*. 3020–3026.
- [25] Yiyu Liu, Qian Liu, Yu Tian, Changping Wang, Yanan Niu, Yang Song, and Chenliang Li. 2021. Concept-aware denoising graph neural network for micro-video recommendation. In *Proceedings of the 30th ACM international conference on information & knowledge management*. 1099–1108.
- [26] Hongxu Ma, Kai Tian, Tao Zhang, Xuefeng Zhang, Han Zhou, Chunjie Chen, Han Li, Jihong Guan, and Shuigeng Zhou. 2024. Generative Regression Based Watch Time Prediction for Short-Video Recommendation. *arXiv preprint arXiv:2412.20211* (2024).
- [27] Hongxu Ma, Guanshuo Wang, Fufu Yu, Qiong Jia, and Shouhong Ding. 2025. Ms-detr: Towards effective video moment retrieval and highlight detection by joint motion-semantic learning. In *Proceedings of the 33rd ACM International Conference on Multimedia*. 4514–4523.
- [28] Hongxu Ma, Chenbo Zhang, Lu Zhang, Jiaogen Zhou, Jihong Guan, and Shuigeng Zhou. 2025. Fine-grained zero-shot object detection. In *Proceedings of the 33rd ACM International Conference on Multimedia*. 4504–4513.
- [29] Hongxu Ma, Han Zhou, Kai Tian, Xuefeng Zhang, Chunjie Chen, Han Li, Jihong Guan, and Shuigeng Zhou. 2026. GoR: The Fourteenth and Extensible Generative Framework for Ordinal Regression. In *The Fifteenth International Conference on Learning Representations*. <https://openreview.net/forum?id=ys80cc2N5M>
- [30] George Papamakarios, Eric Nalisnick, Danilo Jimenez Rezende, Shakir Mohamed, and Balaji Lakshminarayanan. 2021. Normalizing flows for probabilistic modeling and inference. *J. Mach. Learn. Res.* 22, 1, Article 57 (Jan. 2021), 64 pages.
- [31] Danilo Rezende and Shakir Mohamed. 2015. Variational inference with normalizing flows. In *International conference on machine learning*. PMLR, 1530–1538.
- [32] Fei Sun, Jun Liu, Jian Wu, Changhua Pei, Xiao Lin, Wenwu Ou, and Peng Jiang. 2019. BERT4Rec: Sequential recommendation with bidirectional encoder representations from transformer. In *Proceedings of the 28th ACM international conference on information and knowledge management*. 1441–1450.
- [33] Jie Sun, Zhaoying Ding, Xiaoshuang Chen, Qi Chen, Yincheng Wang, Kaiqiao Zhan, and Ben Wang. 2024. CREAD: A Classification-Restoration Framework with Error Adaptive Discretization for Watch Time Prediction in Video Recommender Systems. In *Proceedings of the AAAI Conference on Artificial Intelligence*.
- [34] Siqi Wu, Marian-Andrei Rizoiu, and Lexing Xie. 2018. Beyond views: Measuring and predicting engagement in online videos. In *Proceedings of the International AAAI Conference on Web and Social Media*, Vol. 12.
- [35] Tingyu Wu, Zhisheng Chen, Ziyang Wang, Shuhe Wang, Chenglong Li, Shuo Zhang, Sen Hu, Silin Wu, Qizhen Lan, Huacan Wang, et al. 2026. KnowMe-Bench: Benchmarking Person Understanding for Lifelong Digital Companions. *arXiv preprint arXiv:2601.04745* (2026).
- [36] Shentao Yang, Haichuan Yang, Linna Du, Adithya Ganesh, and et al. 2024. SwAT: Statistical Modeling of Video Watch Time through User Behavior Analysis. *arXiv preprint arXiv:2408.07759* (2024). doi:10.48550/arXiv.2408.07759
- [37] Zhengyi Yang, Jiancan Wu, Zhicai Wang, Xiang Wang, Yancheng Yuan, and Xiangnan He. 2023. Generate what you prefer: Reshaping sequential recommendation via guided diffusion. *Advances in Neural Information Processing Systems* 36 (2023), 24247–24261.
- [38] Xing Yi, Liangjie Hong, Erheng Zhong, Nanthan Nan Liu, and Suju Rajan. 2014. Beyond clicks: dwell time for personalization. In *Proceedings of the 8th ACM Conference on Recommender systems*. 113–120.
- [39] Yuanqing Yu, Chongming Gao, Jiawei Chen, Heng Tang, Yuefeng Sun, Qian Chen, Weizhi Ma, and Min Zhang. 2024. EasyRL4Rec: An Easy-to-use Library for Reinforcement Learning Based Recommender Systems. *arXiv e-prints*, Article arXiv:2402.15164 (Feb. 2024), arXiv:2402.15164 pages. arXiv:2402.15164 [cs.IR] doi:10.48550/arXiv.2402.15164
- [40] Ruohan Zhan, Changhua Pei, Qiang Su, Jianfeng Wen, Xueliang Wang, Guanyu Mu, Dong Zheng, Peng Jiang, and Kun Gai. 2022. Deconfounding duration bias in watch-time prediction for video recommendation. In *Proceedings of the 28th ACM SIGKDD Conference on Knowledge Discovery and Data Mining*. 4472–4481.
- [41] Chenbo Zhang, Bing Huangfu, Hongxu Ma, Jihong Guan, and Shuigeng Zhou. 2025. Multi-modal Prototype Guided Few-shot Object Detection. In *Proceedings of the 33rd ACM International Conference on Multimedia*. 1852–1861.
- [42] Haiyuan Zhao, Guohao Cai, Jieming Zhu, Zhenhua Dong, Jun Xu, and Ji-Rong Wen. 2024. Counteracting Duration Bias in Video Recommendation via Counterfactual Watch Time. In *Proceedings of the 30th ACM SIGKDD Conference on Knowledge Discovery and Data Mining*. 4455–4466.
- [43] Haiyuan Zhao, Lei Zhang, Jun Xu, Guohao Cai, Zhenhua Dong, and Ji-Rong Wen. 2023. Uncovering user interest from biased and noised watch time in video recommendation. In *Proceedings of the 17th ACM Conference on Recommender Systems*. 528–539.

- [44] Xu Zhao, Ruibo Ma, Jiaqi Chen, Weiqi Zhao, Ping Yang, and Yao Hu. 2025. Multi-Granularity Distribution Modeling for Video Watch Time Prediction via Exponential-Gaussian Mixture Network. In *Proceedings of the Nineteenth ACM Conference on Recommender Systems*. 309–318.
- [45] Lijing Zhu, Qizhen Lan, Qing Tian, Wenbo Sun, Li Yang, Lu Xia, Yixin Xie, Xi Xiao, Tieshang Duan, Cui Tao, et al. 2025. ETT-CKGE: Efficient Task-Driven Tokens for Continual Knowledge Graph Embedding. In *Joint European Conference on Machine Learning and Knowledge Discovery in Databases*. Springer, 481–496.

A Theoretical Proofs

A.1 Limitations in Ordinal Regression Methods: A Case Study with CREAD

This section provides a theoretical analysis of these limitations, demonstrating the importance of capturing temporal dependencies to improve prediction accuracy. We quantify this error using the Kullback-Leibler (KL) divergence between the true sequential probability distribution and the naive approximation that assumes conditional independence.

Let $\{(x_i, y_i)\}_{i=1}^N$ be the training set, where $y_i \in \mathbb{R}$ is the ground-truth watch time, and $x_i \in \mathbb{R}^d$ denotes the i -th input feature vector integrating user- and item-side features. Discretized ordinal regression methods operate by discretizing the continuous range of y using M thresholds, $c_1 < c_2 < \dots < c_M$, which define a set of intervals.

Instead of modeling the probability of y_i falling into a specific interval, these methods model a sequence of binary decisions. We define a sequence of Bernoulli random variables $\mathbf{B}_i = (\mathbf{B}_i^1, \dots, \mathbf{B}_i^M)$ for each data point i , where:

$$\mathbf{B}_i^m = 1(y_i > c_m) \quad (26)$$

Here, $1(\cdot)$ is the indicator function, and $\mathbf{B}_i^m = 1$ represents the event that the true value y_i exceeds the threshold c_m . The prediction \hat{y}_i is then constructed as a weighted sum of the probabilities of these binary events.

The naive CREAD model implicitly assumes conditional independence across discretized intervals:

$$P_{\text{naive}}(\mathbf{B}_i | x_i) = \prod_{m=1}^M P(\mathbf{B}_i^m | x_i). \quad (27)$$

However, these decisions are inherently dependent. The knowledge that y_i has surpassed a threshold c_{m-1} (i.e., $\mathbf{B}_i^{m-1} = 1$) provides significant information about whether it will also surpass the next threshold c_m . The true conditional distribution factorizes sequentially:

$$P_{\text{true}}(\mathbf{B}_i | x_i) = \prod_{m=1}^M P(\mathbf{B}_i^m | \mathbf{B}_i^{< m}, x_i), \quad (28)$$

where $\mathbf{B}_i^{< m} = (\mathbf{B}_i^1, \dots, \mathbf{B}_i^{m-1})$ represents the history of binary decisions up to step m .

The information loss or error introduced by the naive model's independence assumption can be precisely quantified by the KL

divergence between the true and naive distributions:

$$\begin{aligned} D_{KL}(P_{\text{true}} \| P_{\text{naive}}) &= \sum_{\mathbf{B}_i} P_{\text{true}}(\mathbf{B}_i | x_i) \log \frac{P_{\text{true}}(\mathbf{B}_i | x_i)}{P_{\text{naive}}(\mathbf{B}_i | x_i)} \\ &= \sum_{\mathbf{B}_i} P_{\text{true}}(\mathbf{B}_i | x_i) \log \frac{\prod_{m=1}^M P(\mathbf{B}_i^m | \mathbf{B}_i^{< m}, x_i)}{\prod_{m=1}^M P(\mathbf{B}_i^m | x_i)} \quad (29) \\ &= \sum_{\mathbf{B}_i} P_{\text{true}}(\mathbf{B}_i | x_i) \sum_{m=1}^M \log \frac{P(\mathbf{B}_i^m | \mathbf{B}_i^{< m}, x_i)}{P(\mathbf{B}_i^m | x_i)} \end{aligned}$$

Rearranging the summation terms, we derive the total KL divergence that quantifies the error introduced by ignoring dependencies among discretized intervals:

$$\begin{aligned} D_{KL}(P_{\text{true}} \| P_{\text{naive}}) &= \sum_{m=1}^M \sum_{\mathbf{B}_i} P_{\text{true}}(\mathbf{B}_i | x_i) \log \frac{P(\mathbf{B}_i^m | \mathbf{B}_i^{< m}, x_i)}{P(\mathbf{B}_i^m | x_i)} \\ &= \sum_{m=1}^M \mathbb{E}_{\mathbf{B}_i \sim P_{\text{true}}} \left[\log \frac{P(\mathbf{B}_i^m | \mathbf{B}_i^{< m}, x_i)}{P(\mathbf{B}_i^m | x_i)} \right] \quad (30) \\ &= \sum_{m=1}^M \mathbb{E}_{\mathbf{B}_i^{< m}} \left[D_{KL}^{(m)} \right] \end{aligned}$$

This can be explicitly expressed as the conditional KL divergence for each bucket:

$$\begin{aligned} D_{KL}^{(m)} &= D_{KL}(P(\mathbf{B}_i^m | x_i, \mathbf{B}_i^{< m}) \| P(\mathbf{B}_i^m | x_i)) \\ &= \sum_{b^m \in \{0,1\}} P(\mathbf{B}_i^m = b^m | x_i, \mathbf{B}_i^{< m}) \log \frac{P(\mathbf{B}_i^m = b^m | x_i, \mathbf{B}_i^{< m})}{P(\mathbf{B}_i^m = b^m | x_i)} \quad (31) \end{aligned}$$

This expectation can be approximated as:

$$\mathbb{E}_{\mathbf{B}_i^{< m}} \left[D_{KL}^{(m)} \right] \approx I(\mathbf{B}_i^m; \mathbf{B}_i^{< m} | x_i) \quad (32)$$

where $I(\mathbf{B}_i^m; \mathbf{B}_i^{< m} | x_i)$ denotes the conditional mutual information between the current decision \mathbf{B}_i^m and all preceding decisions $\mathbf{B}_i^{< m}$, given the features x_i . The detailed proof is in the following:

$$\begin{aligned} I(\mathbf{B}_i^m; \mathbf{B}_i^{< m} | x_i) &\triangleq \sum_{\mathbf{b}^{< m}, b^m} P(\mathbf{b}^{< m}, b^m | x_i) \log \frac{P(b^m | \mathbf{b}^{< m}, x_i)}{P(b^m | x_i)} \\ &= \sum_{\mathbf{b}^{< m}} P(\mathbf{b}^{< m} | x_i) \sum_{b^m} P(b^m | \mathbf{b}^{< m}, x_i) \log \frac{P(b^m | \mathbf{b}^{< m}, x_i)}{P(b^m | x_i)} \\ &= \sum_{\mathbf{b}^{< m}} P(\mathbf{b}^{< m} | x_i) (D_{KL}(P(\mathbf{B}_i^m | x_i, \mathbf{B}_i^{< m}) \| P(\mathbf{B}_i^m | x_i))) \\ &\triangleq \mathbb{E}_{\mathbf{B}_i^{< m} \sim P(\cdot | x_i)} \left[D_{KL}^{(m)} \right] \quad (33) \end{aligned}$$

The derived KL divergence decomposition illustrates that the error introduced by the naive discretized modeling approach which ignores dependencies across intervals, can be quantified precisely as the cumulative sum of conditional mutual information across all discretized intervals. Specifically, if intervals are entirely independent (i.e., mutual information $I = 0$), the resulting KL divergence error is zero; conversely, if strong dependencies exist among intervals ($I > 0$), the error increases proportionally to the strength of these dependencies.

A.2 Mean Collapse in Regression

PROOF. Step 1: Optimal Solution Derivation. The objective is $\min_f \mathbb{E}_{x,y} [\|y - f(x)\|^2]$. Setting the functional derivative to zero:

$$\frac{\delta}{\delta f} \int \int (y-f(x))^2 p_{\text{data}}(y|x)p(x)dydx = 0 \implies f^*(x) = \mathbb{E}_{p_{\text{data}}} [y|x]. \quad (34)$$

Under a Gaussian Mixture Model (GMM) representation of p_{data} with modes μ_k :

$$f^*(x) = \sum_{k=1}^K \pi_k(x) \int y \mathcal{N}(y; \mu_k, \sigma^2) dy = \sum_{k=1}^K \pi_k(x) \mu_k(x). \quad (35)$$

Step 2: Density Analysis in Bimodal Case. Consider $K = 2$ with $\pi_1 = \pi_2 = 0.5$. The prediction is the centroid $\bar{\mu} = \frac{\mu_1 + \mu_2}{2}$. The true density at $\bar{\mu}$ is:

$$p_{\text{data}}(\bar{\mu}|x) = 0.5 \mathcal{N}(\bar{\mu}; \mu_1, \sigma^2) + 0.5 \mathcal{N}(\bar{\mu}; \mu_2, \sigma^2) \quad (36)$$

$$= \frac{1}{\sqrt{2\pi}\sigma} \exp\left(-\frac{(\mu_1 - \mu_2)^2}{8\sigma^2}\right). \quad (37)$$

Let $\Delta = |\mu_1 - \mu_2|$. Under the disjoint modes assumption ($\Delta \gg \sigma$), the term $\frac{\Delta^2}{8\sigma^2} \rightarrow \infty$, thus:

$$\lim_{\Delta/\sigma \rightarrow \infty} p_{\text{data}}(f^*(x)|x) = 0. \quad (38)$$

The regression model predicts a value with vanishingly small likelihood, effectively collapsing onto an invalid mean. \square

A.3 Latent Space Partitioning and NF-Driven Generation

We study a continuous generative regression model with latent variable $z \in \mathbb{R}^d$ and conditional decoder mean $\mu_\theta(z, x)$, where x denotes observed conditioning features and $\{\alpha_k\}_{k=1}^K$ denotes the dominant modes of the true conditional distribution $p_{\text{data}}(y|x)$. For each $k \in \{1, \dots, K\}$, the decoder-induced region are assumed to be pairwise disjoint, defined as:

$$\mathcal{Z}_k \triangleq \{z : \|\mu_\theta(z, x) - \alpha_k\| \leq \varepsilon\}. \quad (39)$$

PROPOSITION 5 (DECODER-INDUCED LATENT PARTITION). Assume $\mu_\theta(\cdot, x)$ is L -Lipschitz with respect to z :

$$\|\mu_\theta(z_1, x) - \mu_\theta(z_2, x)\| \leq L\|z_1 - z_2\|, \quad \forall z_1, z_2. \quad (40)$$

Let $\Delta \triangleq \min_{i \neq j} \|\alpha_i - \alpha_j\|$. If $\Delta > 2\varepsilon$, then $\mathcal{Z}_i \cap \mathcal{Z}_j = \emptyset$ for all $i \neq j$. Moreover, for any $z_i \in \mathcal{Z}_i$ and $z_j \in \mathcal{Z}_j$ with $i \neq j$,

$$\|z_i - z_j\| \geq \frac{\Delta - 2\varepsilon}{L}. \quad (41)$$

PROOF. Fix any $i \neq j$ and take arbitrary $z_i \in \mathcal{Z}_i$ and $z_j \in \mathcal{Z}_j$. By the triangle inequality,

$$\begin{aligned} \|\mu_\theta(z_i, x) - \mu_\theta(z_j, x)\| &\geq \|\alpha_i - \alpha_j\| - \|\mu_\theta(z_i, x) - \alpha_i\| - \|\mu_\theta(z_j, x) - \alpha_j\| \\ &\geq \|\alpha_i - \alpha_j\| - 2\varepsilon \geq \Delta - 2\varepsilon. \end{aligned} \quad (42)$$

By the Lipschitz condition (40), $\|z_i - z_j\| \geq \frac{1}{L} \|\mu_\theta(z_i, x) - \mu_\theta(z_j, x)\| \geq \frac{\Delta - 2\varepsilon}{L}$, which proves (41). If $\Delta > 2\varepsilon$ and $\mathcal{Z}_i \cap \mathcal{Z}_j \neq \emptyset$, then there exists $z \in \mathcal{Z}_i \cap \mathcal{Z}_j$, implying $\|\mu_\theta(z, x) - \alpha_i\| \leq \varepsilon$ and $\|\mu_\theta(z, x) - \alpha_j\| \leq \varepsilon$. Thus $\|\alpha_i - \alpha_j\| \leq 2\varepsilon$, contradicting $\Delta > 2\varepsilon$. Hence $\mathcal{Z}_i \cap \mathcal{Z}_j = \emptyset$. \square

PROPOSITION 6 (COVERAGE IMPLIES MODE-CONSISTENT DECODING). Let $p(z|c)$ be any conditional sampling distribution and define its coverage over decoder-induced regions by

$$\alpha(c) \triangleq \mathbb{P}_{p(\cdot|c)} \left(z \in \bigcup_{k=1}^K \mathcal{Z}_k \right) = \sum_{k=1}^K \mathbb{P}_{p(\cdot|c)} (z \in \mathcal{Z}_k). \quad (43)$$

Define the decoding-success event

$$E \triangleq \left\{ \min_{1 \leq k \leq K} \|\mu_\theta(z, x) - \alpha_k\| \leq \varepsilon \right\}, \quad \mathbb{P}(E|c) \geq \alpha(c). \quad (44)$$

PROOF. If $z \in \bigcup_{k=1}^K \mathcal{Z}_k$, then by the definition of union there exists some $k \in \{1, \dots, K\}$ such that $z \in \mathcal{Z}_k$. By equation 39, $z \in \mathcal{Z}_k$ implies $\|\mu_\theta(z, x) - \alpha_k\| \leq \varepsilon$. Therefore, $\min_{1 \leq j \leq K} \|\mu_\theta(z, x) - \alpha_j\| \leq \|\mu_\theta(z, x) - \alpha_k\| \leq \varepsilon$, which means $z \in E$ by the definition of E in (44). Hence, $\{z \in \bigcup_{k=1}^K \mathcal{Z}_k\} \subseteq E$. Taking probability under $p(z|c)$ and using the monotonicity of probability measures yields

$$\mathbb{P}(E|c) \geq \mathbb{P} \left(z \in \bigcup_{k=1}^K \mathcal{Z}_k \mid c \right) = \alpha(c). \quad (45)$$

\square

A.3.1 NF Pullback Mass and Partition Selection.

Assumption 1 (NF Mass Concentration). Let $\varepsilon \sim \mathcal{N}(0, I)$ and $z = f_\psi(\varepsilon; c)$ be an invertible Normalizing Flow parameterized by ψ , conditioned on context c . Let $\delta \in (0, 1)$ be a tolerance parameter. Assume that for the given context c there exists an index $k(c) \in \{1, \dots, K\}$ such that

$$\int_{f_\psi^{-1}(\mathcal{Z}_{k(c)}; c)} \mathcal{N}(\varepsilon; 0, I) d\varepsilon \geq 1 - \delta. \quad (46)$$

PROPOSITION 7 (NF COVERAGE UNDER ASSUMPTION 1). Let $p_\psi(z|c)$ denote the conditional distribution induced by the Normalizing Flow $f_\psi(\cdot; c)$. Define the NF coverage as

$$\alpha_{\text{NF}}(c) \triangleq \mathbb{P}_{p_\psi(\cdot|c)} \left(z \in \bigcup_{k=1}^K \mathcal{Z}_k \right) = \sum_{k=1}^K \mathbb{P}_{p_\psi(\cdot|c)} (z \in \mathcal{Z}_k). \quad (47)$$

Under Assumption 1, the coverage satisfies

$$\alpha_{\text{NF}}(c) \geq 1 - \delta. \quad (48)$$

PROOF. Since $z = f_\psi(\varepsilon; c)$ is an invertible measurable map, for any measurable set $S \subseteq \mathbb{R}^d$ we have the change-of-variables identity

$$\mathbb{P}_{p_\psi(\cdot|c)} (z \in S) = \mathbb{P}(\varepsilon \in f_\psi^{-1}(S; c)) = \int_{f_\psi^{-1}(S; c)} \mathcal{N}(\varepsilon; 0, I) d\varepsilon. \quad (49)$$

In particular, for each decoder-induced region \mathcal{Z}_k ,

$$\mathbb{P}_{p_\psi(\cdot|c)} (z \in \mathcal{Z}_k) = \int_{f_\psi^{-1}(\mathcal{Z}_k; c)} \mathcal{N}(\varepsilon; 0, I) d\varepsilon. \quad (50)$$

By definition (47) and non-negativity of probabilities, $\alpha_{\text{NF}}(c) = \sum_{k=1}^K \mathbb{P}_{p_\psi(\cdot|c)} (z \in \mathcal{Z}_k) \geq \mathbb{P}_{p_\psi(\cdot|c)} (z \in \mathcal{Z}_{k(c)})$. Applying (50) with $k = k(c)$ and using Assumption 1 yields

$$\alpha_{\text{NF}}(c) \geq \int_{f_\psi^{-1}(\mathcal{Z}_{k(c)}; c)} \mathcal{N}(\varepsilon; 0, I) d\varepsilon \geq 1 - \delta. \quad (51)$$

\square

We introduce an explicit *conditional assumption*: given a context c , the NF, during inference-time sampling, concentrates its probability mass (up to a tolerance δ) on a single latent partition implicitly induced by the decoder. Under this assumption, we establish a rigorous probabilistic guarantee: the probability that NF sampling falls into a latent region that can be decoded into a true conditional mode is at least $1 - \delta$. This result formalizes the role of NF in our framework: it acts as a *geometry-aware sampling mechanism* that, without participating in training or regularization, reliably steers generation toward high-density output modes already captured by the decoder.

PROPOSITION 8 (GENERATION CONSISTENCY UNDER NF SAMPLING). *Assume the conditions of Proposition 5. Let $\hat{z} \sim p_{\psi}(z | c)$ and $\hat{y} = \mu_{\theta}(\hat{z}, x)$. If Proposition 7 holds with parameter δ , then*

$$\mathbb{P}\left(\min_{1 \leq k \leq K} \|\hat{y} - \alpha_k\| \leq \varepsilon \mid c\right) \geq 1 - \delta. \quad (52)$$

PROOF. By Proposition 6, $\mathbb{P}(E | c) \geq \alpha_{\text{NF}}(c)$. By Proposition 7, $\alpha_{\text{NF}}(c) \geq 1 - \delta$. Combining yields $\mathbb{P}(E | c) \geq 1 - \delta$. Finally, E is exactly the event $\min_k \|\mu_{\theta}(\hat{z}, x) - \alpha_k\| \leq \varepsilon$, and $\hat{y} = \mu_{\theta}(\hat{z}, x)$ completes the proof. \square

This proposition shows that once the decoder induces mode-aligned latent partitions, it suffices for the Normalizing Flow to select any one of these partitions with high probability during sampling; the generated output will then fall into the corresponding high-density mode of the true conditional distribution with the same probability, ensuring consistent and non-averaged generation.

A.4 Proof of AR Limitations

We provide a bias variance decomposition of the expected squared regression error for tokenized AR models following [29].

Setup and Notation. Consider a continuous target reconstructed from a sequence of value tokens: $y \triangleq \sum_{t=1}^T \phi(s^t)$, where s^t denotes the ground-truth token at step t and $\phi(\cdot)$ maps a token to its numeric value. The AR model predicts a token sequence $\hat{s}^{1:T}$, yielding the prediction $\hat{y} \triangleq \sum_{t=1}^T \phi(\hat{s}^t)$.

Define the numeric token values $C^t \triangleq \phi(s^t)$, $\hat{C}^t \triangleq \phi(\hat{s}^t)$, and the step-wise prediction error $\Delta_t \triangleq \hat{C}^t - C^t$. By assumption, all token values are bounded: $C^t, \hat{C}^t \in [w_{\min}, w_{\max}]$, and the step-wise bias satisfies $|\mathbb{E}[\Delta_t]| \leq B, \forall t$.

Error Decomposition. The squared regression error can be written as

$$\mathbb{E}[(\hat{y} - y)^2] = \mathbb{E}\left[\left(\sum_{t=1}^T \Delta_t\right)^2\right]. \quad (53)$$

Using the bias-variance decomposition, we obtain

$$\mathbb{E}\left[\left(\sum_{t=1}^T \Delta_t\right)^2\right] = \left(\sum_{t=1}^T \mathbb{E}[\Delta_t]\right)^2 + \mathbb{V}\left(\sum_{t=1}^T \Delta_t\right). \quad (54)$$

Bias Term. Let $b_t \triangleq \mathbb{E}[\Delta_t]$. Since $|b_t| \leq B$, we have

$$\left(\sum_{t=1}^T b_t\right)^2 \leq T^2 B^2. \quad (55)$$

Variance Term. The variance term expands as

$$\mathbb{V}\left(\sum_{t=1}^T \Delta_t\right) = \sum_{t=1}^T \mathbb{V}(\Delta_t) + \sum_{t \neq t'} \text{Cov}(\Delta_t, \Delta_{t'}). \quad (56)$$

Applying the Cauchy-Schwarz inequality yields

$$\sum_{t \neq t'} \text{Cov}(\Delta_t, \Delta_{t'}) \leq \frac{T(T-1)}{2} \max_t \mathbb{V}(\Delta_t). \quad (57)$$

Since $\Delta_t = \hat{C}^t - C^t$ and both \hat{C}^t and C^t lie in $[w_{\min}, w_{\max}]$, Popoviciu's inequality gives

$$\mathbb{V}(\Delta_t) \leq \frac{(w_{\max} - w_{\min})^2}{4}. \quad (58)$$

Therefore,

$$\mathbb{V}\left(\sum_{t=1}^T \Delta_t\right) \leq T^2 \cdot \frac{(w_{\max} - w_{\min})^2}{4}. \quad (59)$$

Final Bound. Combining the bias and variance bounds, we obtain

$$\mathbb{E}[(\hat{y} - y)^2] \leq T^2 B^2 + T^2 \frac{(w_{\max} - w_{\min})^2}{4}. \quad \square \quad (60)$$

Vocabulary-induced trade-off. Both the sequence length T and the step-wise bias bound B are induced by the vocabulary design. Let \mathcal{V} denote the value-token vocabulary and $\phi(\mathcal{V}) \subset [w_{\min}, w_{\max}]$ its numeric range. A finer-grained vocabulary yields smaller token magnitudes and typically requires a longer sequence to represent the same target, leading to larger T . Conversely, a coarser vocabulary reduces T but increases discretization error at each step, enlarging the attainable bias bound B . In particular, since $\Delta_t = \phi(\hat{s}^t) - \phi(s^t)$ and $\phi(s^t), \phi(\hat{s}^t) \in [w_{\min}, w_{\max}]$, we have $|\Delta_t| \leq w_{\max} - w_{\min} \Rightarrow |\mathbb{E}[\Delta_t]| \leq B \leq w_{\max} - w_{\min}$. Therefore, tokenized AR regression is intrinsically constrained by a vocabulary-dependent trade-off between T and B , which directly controls the error bound in Proposition 3.